ON THE INFLUENCE OF SPECIMEN ORIENTATION ON THE DUCTILE FRACTURE BEHAVIOUR OF THE STEEL Fe E 350

D. Dormagen and W. Dahl

Institute of Ferrous Metallurgy, Technical University of Aachen, Federal Republic of Germany

ABSTRACT

For 125 mm thick plate Fe E 350 tests were carried out with notched and smooth round bars, flat tensile bars, Charpy - V-notch and CT-specimens in the L-T, T-L, and S-L orientation. The decrease in fracture properties is due to lamellar tearing characterized by sulfide accumulated terraces influencing the stress state at the crack tip and the void formation in the fracture surface.

KEYWORDS

Deformation behaviour, fracture initiation and propagation in L-T, T-L and S-L orientation, SEM studies and statistical fracture surface analysis.

INTRODUCTION

The necessity to establish the safety of structures operating in a regime where the material behaviour is fully ductile has le to an interest in the micromechanisms of ductile fracture and to their relationships with fracture mechanics parameters such as J-Integral or crack opening displacement CTOD. As ductile fracture is characterized by void coalescence the volume fraction, shape and distribution of Mn-sulfides in the steel-matrix can influence the fracture behaviour of structural steels.

Early studies (Dahl, 1977; Dahl and others, 1966; Fuchs and others, 1975) have shown the influence of sulfur content on the anisotropy of the fracture behaviour in notched bar impact bend tests. With increasing volume fraction of sulfides the upper shel values decrease especially in the S-L direction due to the location of the elongated Mn-sulfides in the steel-matrix. This anisotropy can be removed by lowering the sulfur content and have demonstrated the influence of sulfide-distribution and sulfide-shape on the onset of stable crack growth and the J-Resistance-

Curve (Laintridou and Pineau, 1982). The values in the S-L orientation are lower concerning crack initiation and the slope of the R-curve. Green (1982) presented a quantitative model describing the influence of shape and distribution of sulfides on the stress and strain field ahead of a crack tip. As anisotropic material behaviour has been observed in sulfide-shape controlled steel (Wilson, 1979) as well, deformation textures must be therefore taken into account, too.

MATERIAL CHARACTERIZATION

In this paper the influence of specimen orientation on the deformation and fracture behaviour of normalized, 125 mm thick plates of the steel Fe E 350 is investigated. In Fig. 1 the chemical composition, the heat treatment and the microstructure is presented. The material is characterized by a ferritic-pearlitic microstructure with no pronounced banding. Grain sizes are independent of specimen-orientation and not elongated in the rolling direction. The mean ferrite grain size was determined to d_m = 6 - 7 µm. The microscopic pictures show Mn-sulfides of Type II, but according to the plate thickness of 125 mm the characteristic forms of elongated MnS-inclusions are missing. Because of the lower hardness in the middle of the plate and because of some segregation bands at 1/5-th of the plate thickness B all specimens were taken from the mid-thickness position.

Steel: Fe E 350

normalized

chemical composition

C	Si	Mn	P	S	Cr	Cu	Al	V	Ni
0,13	0,33	1,44	0,010	0,016	0,05	0,08	0,018	0,16	0,01

microstructure

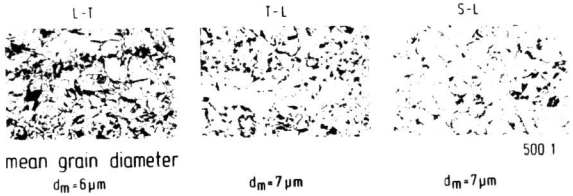

mean grain diameter

d_m=6µm d_m=7µm d_m=7µm

Fig. 1. Chemical composition and microstructure of steel Fe E 350

TESTING CONDITIONS

In order to investigate the deformation- and fracture behaviour, tests were carried out with notched and smooth round bars, flat tensile bars, with Charpy-V-notch and CT-specimens. By the different tests the material behaviour is investigated under uniaxial and multi-axial stress conditions. Fracture toughness properties are determined to characterize the crack initiation and propagation behaviour. The tests were carried out for the L-T, T-L and S-L orientation.

Scanning electron microscope studies and statistical fracture surface analysis were made to explain the material's anisotropic behaviour.

RESULTS

In Fig. 2 the results of the Charpy-V-notch tests are presented. The transition temperatures for 50 % upper shelf value do not differ very much, but the influence of specimen orientation in the ductile regime of upper shelf is very clearly to be seen. From 168 J in the L-T direction, Charpy-energy decreases to 110 J for T-L specimens and 50 J in the S-L orientation. As the differences are rather big in spite of the low grade of deformation, the texture was analysed and the deformation anisotropy was investigated. Pronounced textures were not measured. The results of the flat tensile test bars according to DIN 50125 are presented in Fig. 3. The anisotropy characterizing r-values were determined in the x-, y and z-direction in the plate edge and midness. All values are slightly lower than one and no differences between the different directions can be seen.

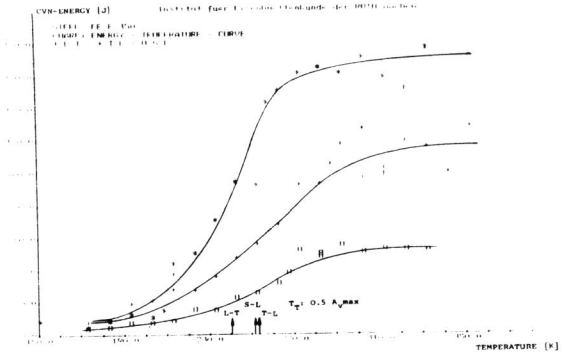

Fig. 2. Charpy-energy as a function of temperature

In order to explain the differences in upper shelf energy values, fracture toughness parameters were determined to characterize the crack initiation and propagation behaviour.

Steel: Fe E 350
normalized
plate thickness B =125mm
flat tensile test bar acc. DIN 50125
L-T and T-L specimen

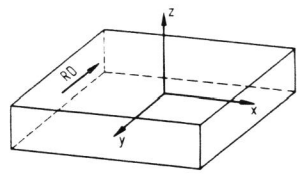

spec. location	r_x	r_y	r_z
plate-edge	0,97	0,97	1,00
plate-midness	0,96	0,95	0,99

$$r_y = \frac{\beta}{D}\Big|_L \qquad r_x = \frac{\beta}{D}\Big|_Q \qquad \frac{r_x - r_z}{r_y} = 1$$

Fig. 3. R-values of steel Fe E 350

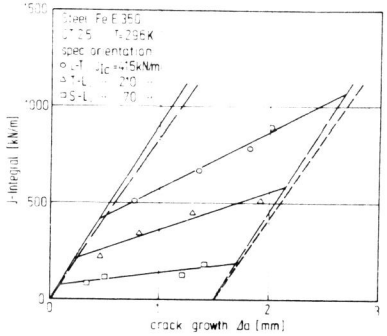

Fig. 4. J_{Ic}-determination according to ASTM E 813

The value of J_{Ic} was determined according ASTM E 813 using CT-25 specimens and the R-curve was derived from the multi-specimen technique using CT-50 specimens. In Fig. 4 the results of the ASTM E 813 procedure are presented. A strong influence of specimen orientation on J_{Ic}-values is to be seen. J_{Ic} decreases from 415 kN/m for the L-T direction to 70 kN/m in the S-L direction. Looking at the slopes of the R-curve in terms of J versus Δa in Fig. 5 the same tendency can be observed. The crack resistance in the L-T orientation is highest and lowest in the S-L direction in the region of J controlled crack growth. Thus the fracture toughness properties are in accordance with the differences in Charpy-energy values when ductile failure occours.

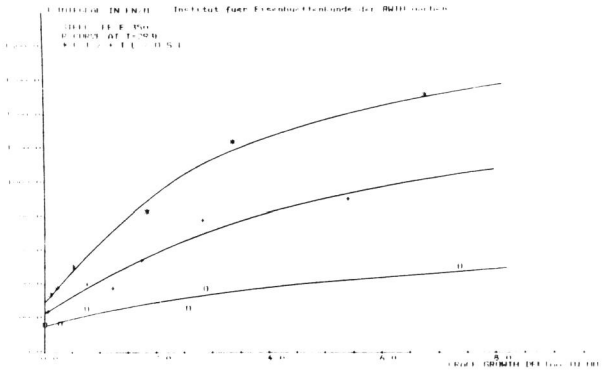

Fig. 5. R-curves of steel Fe E 350 at room temperature

In Fig. 6 the SEM-fracture surfaces of CT-50 specimens are presented for the three orientations at the transition from fatigue crack to stable crack growth.

Steel: Fe E 350
normalized
fracture surface: CT-specimen

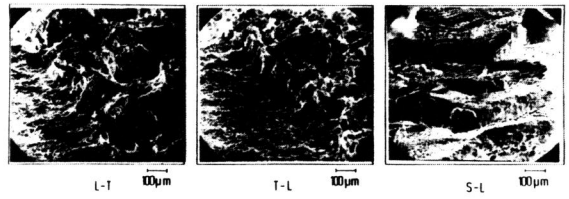

Fig. 6. Fracture surfaces of CT-specimen at the transition from fatigue crack to stable crack growth

In the S-L direction a typical lamellar fracture type is to be seen. The single fracture terrace is characterized not by the typical fibres but by a net-like structure of voids with Mn-sulfides accumulated. The deformation of the voids within the terraces is small compared to the other orientations. The steel-matrix is heavily weakened by this fracture type being responsible for the low energy-consumption when the crack advances. Fracture can easily occur along the interface steel-matrix and sulfides. For the L-T and T-L orientation fracture occurs trans-

verse and longitudinal to these sulfide terraces. Thus the deformation of the matrix is higher resulting in higher dJ/da-values. Detailed studies of the sulfide shape in these terraces have demonstrated a prevailing globular structure of the non metallic inclusions and some platelets were observed parallel and perpendicular to the rolling direction. The manganese-sulfides show a very narrow spacing so that the proportions found in the light microscope are not representing the fracture appearance of S-L specimens. Not regarding the single non-metallic inclusions, but the terrace itself, the statistical analysis of lengths is presented in Fig. 7. The ratio of length in longitudinal and transverse direction was determined to a/b = 1.76. Comparing this result with the ratio of J_{L-T}/J_{T-L} = 1.58 in the regime of J-controlled crack growth the agreement is quite good.

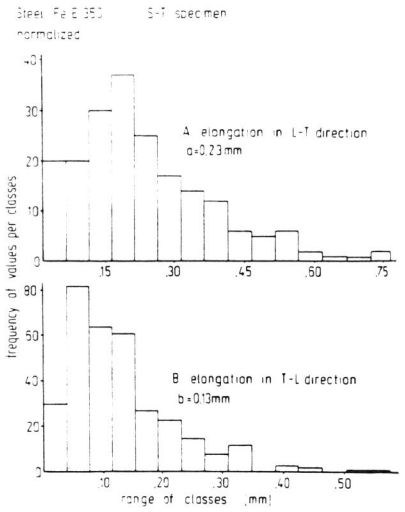

Fig. 7. Statistical analysis of fracture surface

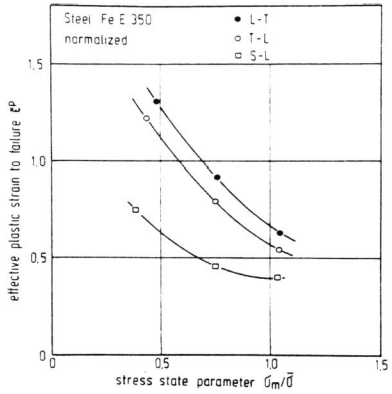

Fig. 8. Effective plastic strain fo failure $\bar{\varepsilon}^P$ as a function of stress state parameter $\sigma_m/\bar{\sigma}$

In order to evaluate the influence of the terraces on the stress state at the crack tip, tests with round notched bars were performed according to MacKenzie(1977). The stress ratio $\sigma_m/\bar{\sigma}$ is supposed to characterize the multi-axial stress conditions with the mean stress σ_m.

$$\sigma_m = \frac{1}{3}(\sigma_1 + \sigma_2 + \sigma_3) \qquad (1)$$

and the equivalent stress $\bar{\sigma}$

$$\bar{\sigma} = \sqrt{\frac{1}{2}\left\{(\sigma_1 - \sigma_2)^2 + (\sigma_2 - \sigma_3)^2 + (\sigma_3 - \sigma_1)^2\right\}} \qquad (2)$$

The equivalent plastic strain $d\bar{\varepsilon}^P$ is given by

$$d\bar{\varepsilon}^P = \sqrt{\frac{2}{9}\left\{(d\varepsilon_1^P - d\varepsilon_2^P)^2 + (d\varepsilon_2^P - d\varepsilon_2^P - d\varepsilon_3^P)^2 + (d\varepsilon_3^P - d\varepsilon_1^P)^2\right\}} \qquad (3)$$

Bridgman's stress analysis (1952) of notched round bars for general yielding conditions was used to calculate

$$\left(\frac{\sigma_m}{\bar{\sigma}}\right)_{max} = \frac{1}{3} + \ln(d/2R + 1) \qquad (4)$$

with
R = radius of the notch
d = radius of the net section

and

$$\bar{\varepsilon}^P = 2 \ln(d_o/d)$$

with
d_o = initial radius
d = actual radius

In Fig. 8 the equivalent plastic strain at fracture is plotted versus stress state parameter $\sigma_m/\bar{\sigma}$. For all specimen orientati the effective plastic strain decreases with increasing triaxiality, which is predicted by Rice and Tracey (1969).

At constant values of $\sigma_m/\bar{\sigma}$ the strain at fracture is bigger fo the L-T orientation than for the T-L and S-L direction. Thus t different grade of deformation in the fracture surfaces of Fig characterized by the dimple size and the height of the dimple can be understood in a more quantitative manner.

DISCUSSION

The SEM-studies have demonstrated that material properties suc as Charpy-energy and fracture toughness properties strongly depend on specimen orientation. The influence of non-metallic inclusions on the fracture behaviour is similar in impact bend a fracture mechanics tests. The prediction of theory on the influ of stress state on the effective plastic strains at failure is confirmed.

The material properties which are responsible for the behaviou in the ductile regime are determined therefore by the plastic strains which have to be measured as a function of the state o stress. The local processes ahead of the crack tip are influenced by the distribution of sulfides and are responsible for th different energy consumption.

REFERENCES

Bridgman, P.W. (1952), in: Studies in Large Plastic Flow and Fracture, Mc Graw Hill
Dahl, W. (1977), Material Science Fundamentals on the Behaviou of Sulfur in Steel, Stahl und Eisen, 97, 402 - 424

Dahl, W., H. Hengstenberg and C. Düren (1966), Behaviour of different Types of Sulfides during Shaping and their Effect on Mechanical Properties, Stahl und Eisen, 97, 796 - 817
Fuchs, A. and others (1975), Assessment of the Effect of Sulfides on the Fracture Behaviour of Structural Steel, Arch. Eisenhüttenwesen, 46, 127
Green, G. (1982), Effects of Orientation on Ductile Crack Initiation and Growth. A Comparison of Experiment with Crack Tip Models, EGF 4, Leoben
Laintridou, J.C. and A. Pineau (1982), Crack Initiation and Stable Crack Growth Resistance in 508 Steels in Relation to Inclusion Distribution, Eng. Fract. Mech., 15, 55 - 71
MacKenzie, A.C., J.W. Hancock and K.D. Brown (1977), On the Influence of State of Stress on Ductile Failure Initiation in High Strength Steels, Eng. Fract. Mech., 7, 167 - 188
Rice, J.R. and D.M. Tracey (1969), J. Mech. Phys. Solids, 17, 201 - 217
Willoughby, R.D. and P.L. Pratt (1978), The Effect of Specimen Orientation on the R-Curve, Int. Journ. Fract., 14, 249 - 251
Wilson, A.D. (1979), Characterization of Plate Steels Quality Using Various Toughness Measurement Techniques, ASTM STP 668, 469 - 493